

Communication

New Design of a Sample Cell for Neutron Reflectometry in Liquid–Liquid Systems and Its Application for Studying Structures at Air–Liquid and Liquid–Liquid Interfaces

Kazuhiro Akutsu-Suyama ^{1,*}, Norifumi L. Yamada ², Yuki Ueda ³, Ryuhei Motokawa ³
and Hirokazu Narita ⁴

- ¹ Neutron Science and Technology Center, Comprehensive Research Organization for Science and Society (CROSS), Tokai, Naka 319-1106, Ibaraki, Japan
- ² Neutron Science Laboratory, Center for Integrative Quantum Beam Science, High Energy Accelerator Research Organization, Tokai, Naka 319-1106, Ibaraki, Japan; norifumi.yamada@kek.jp
- ³ Materials Sciences Research Center, Japan Atomic Energy Agency (JAEA), Tokai, Naka 391-1195, Ibaraki, Japan; ueda.yuki@jaea.go.jp (Y.U.); motokawa.ryuhei@jaea.go.jp (R.M.)
- ⁴ Global Zero Emission Research Center, National Institute of Advanced Industrial Science and Technology, Umezono, Tsukuba 305-8569, Ibaraki, Japan; hirokazu-narita@aist.go.jp
- * Correspondence: k_akutsu@cross.or.jp; Tel.: +81-29-219-5300

Abstract: Knowledge of interfacial structures in liquid–liquid systems is imperative, especially for improving two-phase biological and chemical reactions. Therefore, we developed a new sample cell for neutron reflectometry (NR), which enables us to observe the layer structure around the interface, and investigated the adsorption behavior of a typical surfactant, sodium dodecyl sulfate (SDS), on the toluene-*d*₈-D₂O interface under the new experimental conditions. The new cell was characterized by placing the PTFE frame at the bottom to produce a smooth interface and downsized compared to the conventional cell. The obtained NR profiles were readily analyzable and we determined a slight difference in the SDS adsorption layer structure at the interface between the toluene-*d*₈-D₂O and air-D₂O systems. This could be owing to the difference in the adsorption behavior of the SDS molecules depending on the interfacial conditions.

Keywords: neutron reflectometry; liquid–liquid interface; air–liquid interface; adsorption structure; sodium dodecyl sulfate



Citation: Akutsu-Suyama, K.; Yamada, N.L.; Ueda, Y.; Motokawa, R.; Narita, H. New Design of a Sample Cell for Neutron Reflectometry in Liquid–Liquid Systems and Its Application for Studying Structures at Air–Liquid and Liquid–Liquid Interfaces. *Appl. Sci.* **2022**, *12*, 1215. <https://doi.org/10.3390/app12031215>

Academic Editor: Angelo Giglia

Received: 10 December 2021

Accepted: 21 January 2022

Published: 24 January 2022

Publisher's Note: MDPI stays neutral with regard to jurisdictional claims in published maps and institutional affiliations.



Copyright: © 2022 by the authors. Licensee MDPI, Basel, Switzerland. This article is an open access article distributed under the terms and conditions of the Creative Commons Attribution (CC BY) license (<https://creativecommons.org/licenses/by/4.0/>).

1. Introduction

The interfaces between two immiscible liquids composed of organic and aqueous solutions are of great importance in many applications, such as in liquid–liquid extraction of metal ions, two-phase biological and catalytic reactions and two-phase electrochemical systems [1–3]. Liquid–liquid extraction, in which a hydrophobic organic solvent and an aqueous solution are used, is one of the most important methods for the separation and purification of target materials such as chemicals and metal ions. To control this extraction reaction, understanding of chemical reactions of the dissolved organic and/or inorganic molecules in each phase and at the interface is required. The former reactions, including complex formations, etc., have been extensively studied. In contrast, since it is difficult to observe the interfacial structure in detail by conventional structural analyses, interfacial phenomena have not been well clarified yet.

Recently, X-ray and neutron reflectometry (XR and NR) techniques have enabled to access the information on the molecular-level structures at interfaces. Schlossman reported some interesting findings for the liquid–liquid interfaces by XR and NR, such as interfacial widths at water–oil interfaces, ordering of surfactants adsorbed to these interfaces, phase transitions and domain formation in surfactant monolayers and interfacial fluctuations coupled across and confined by thin liquid films [4]. Besides, the total-reflection X-ray

absorption fine structure (TR-XAFS) method developed at BL39XU of SPring-8 is useful, in which the enrichment of bromide ions was observed at an *n*-heptane–water interface in the presence of dimethyldipalmitylammonium ions [5]. These developments are important not only from a technological point of view, but also because they provide information on molecular-level structures at the interfaces. In the field of solvent extraction, the interfacial structure and potential of two different lipophilic extractants were determined using a combination of X-ray and neutron reflectivity experiments [1]. The findings revealed that the extractant-enriched interface could repel or attract hard trivalent cations depending on the ligand's nature. Tummino et al. combined NR and electrochemical characterization techniques to investigate the effects of applied electric fields and electrolyte concentration on the interfacial structure of the interface between two immiscible electrolyte solutions (ITIES), including the impacts of an adsorbed lipid layer [6]. This is the first NR-electrochemistry research study related to the interfacial structure of the ITIES. On the other hand, Scoppola et al. have explained how the considerable accumulation of surfactant contaminants at bare oil/water can be studied using X-ray and neutron reflectometry with appropriate contrast settings [7]. These findings show that surfactant impurities may be a limiting factor in studying fundamental oil/water interface processes.

Among the above recent techniques, NR is quite suitable for the analysis of organic molecules distributed across an organic–water interface, since the contrast between solvent and scatterer can be controlled by isotope labeling, such as using deuterium to replace hydrogen in organic molecules [8–11]. However, in general, deuterated organic molecules are expensive and not readily available; therefore, a smaller-size cell that can provide an ideal liquid–liquid interface is valuable to reduce their usage. The development of a universal experimental apparatus that can handle a wide range of solvent combinations, including water/oil, oil/water, oil/acid and oil/base, is another motivation for a new cell design.

We have studied the improvement of a sample cell which was originally proposed in a TR-XAFS study [5], while the cell is not suitable for neutron experiments; some components need to be replaced. Considering that the NR measurement for the adsorption behavior of an organic molecule on the interface in the liquid–liquid system is now developing, it is worthwhile to provide a method for measurement and analytical results using the new cell by NR. Therefore, in this study, we produced a new type of cell suitable for NR measurements and elucidated the adsorption structure of a typical surfactant, sodium dodecyl sulfate (SDS), at the toluene-*d*₈-D₂O interface with the air-D₂O interface for comparison. It is important to note that, up to now, many structural studies of the adsorption behavior of an SDS molecule at the air/water and oil/water interfaces have been conducted utilizing X-ray and neutron reflectivity, vibrational sum frequency scattering and simulation approaches [12–16]. Therefore, in this study, several model fitting analyses were performed by referring to previous research results on the SDS adsorption layer structure.

2. Materials and Methods

2.1. Reagents and Samples

Hydrogenated and deuterated reagents were used in the NR experiments to change the scattering length density (SLD) of the solvents. Reagents: toluene-*h*₈ (99.5%; Sigma-Aldrich, St. Louis, MO, USA), toluene-*d*₈ (99.0%-*d*; Sigma-Aldrich), deuterium oxide (D₂O; 99.0%-*d*; Sigma-Aldrich) and SDS (95.0%; FUJIFILM Wako Pure Chemical Co., Ltd., Richmond, VA, USA). A 10 mM SDS sample solution was prepared by dissolving an appropriate amount of SDS in D₂O.

2.2. Cell Design

A schematic diagram of the new sample cell used for NR measurements is shown in Figure 1. The liquid–liquid interface was prepared inside a cuboid quartz liquid cell (60 mm × 40 mm × 40 mm). A polytetrafluoroethylene (PTFE) frame was placed at the bottom of the cell to maintain a flat and smooth interface with the aqueous liquid.

The interface appeared at the plateau of the convex meniscus of the aqueous phase with respect to the organic phase. The top of the sample cell was capped with a PTFE cap to prevent evaporation of the aqueous and organic solutions and to avoid additional moisture intrusion. The cell was mounted on the reflectometer's sample stage and then an appropriate volume (8.5~9.0 mL, depending on the combination of organic solvent, aqueous solution and surfactant) of aqueous and organic solutions was added to the sample cell in order of the density of the liquid. The thickness of the upper layer was ~3 mm (it depends on the amount of the upper layer solvent) and the neutron beam was injected through the side of the sample cell. The thickness of the upper layer (3 mm) was sufficient for the measurement of the NR data, because the width of the beam slit in front of the sample was 0.17 mm. Note that, in the neutron transmittance measurements of the sample cell system, 20 mL of toluene- d_8 was added to the sample cell to increase the thickness of the upper layer. Because of the problem of neutron transmittance, the solvent of the upper layer must be deuterated to provide high neutron transmittance.

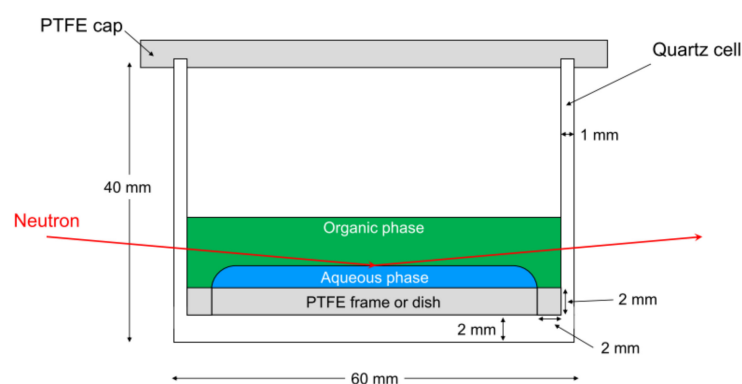


Figure 1. Schematic diagram of the new sample cell for measuring NR. Photos of a new type of cell with the PTFE frame are shown in Figure S1.

2.3. Neutron Transmittance Measurements

Neutron transmittance measurements of the sample cell system were carried out using a neutron reflectometer (BL17 SHARAKU; Tokai, Japan) with a horizontal scattering geometry installed at the Materials and Life Science Experimental Facility (MLF) in J-PARC [17,18]. The incident beam power of the proton accelerator was 600 kW for all the measurements. Pulsed neutron beams were generated in a mercury target at 25 Hz and neutron data were measured using the time-of-flight (TOF) technique. The wavelength (λ) range of the incident neutron beam was tuned to approximately 1.43–8.0 Å for the unpolarized neutron mode by a disk chopper. To maintain a 3 mm \times 3 mm square beam to the sample cell surface, the width of six types of incidence beam slits was set to 3 mm \times 3 mm square. The incident and detector angles were both zero. The TOF neutron data were collected using a ^3He gas tube detector without spatial resolution. All the measurements were taken at ambient temperature. The MLF uses the event recording method as a standard data acquisition system [19]. The data reduction, normalization and subtraction procedures were performed using a program installed in the BL17 SHARAKU system.

2.4. Neutron Reflectometry Measurements

NR measurements were performed using a neutron reflectometer (BL16 SOFIA; Japan) with a vertical scattering geometry installed at the MLF in J-PARC [20,21]. The wavelength range of the incident neutron beam was tuned to approximately 2.2–8.8 Å by a disk chopper. The covered Q_z range was selected as 0.006 or 0.008–0.2 Å $^{-1}$ (the incident angles were 0.3°/0.8°/2.0° or 0.4°/0.9°/2.0°) for air–liquid reflection measurements. On the other hand, the covered Q_z range was selected as 0.016–0.055 Å $^{-1}$ (the incident angle was 0.6°) for liquid–liquid reflection measurements, because large NR data changes were predicted in the area of $Q_z = 0.01\text{--}0.08$ Å $^{-1}$. A 20 mm \times 20 mm beam footprint was maintained on the

sample interface using double-slit collimation. The TOF neutron data were collected by a two-dimensional scintillation detector with spatial resolution. The $\Delta Q_z/Q_z$ resolutions were 5% for the air–liquid reflection measurements and 7% for the liquid–liquid reflection measurements, respectively. The transmitted neutron beam intensity was measured 1 mm above the liquid/liquid interface and the NR data were normalized using the transmitted neutron intensity data. All the measurements were taken at ambient temperature. The data reduction, normalization and subtraction procedures were performed using a program installed in the BL16 SOFIA system. Motofit software [22] was used to fit the NR profiles with a least-squares approach to minimize the deviation of the fit. The thickness (t , Å), SLD (ρ) and Gaussian roughness (σ) values were evaluated using Motofit. On the other hand, the NR data of a limited Q_z -range would have caused ambiguity in the analysis results. Therefore, in order to obtain the thickness of the SDS layer, the thickness and SLD of the SDS layer were constrained to the values optimized manually by referring to previous research works on the SDS adsorption layer structure (these parameters are shown in Tables S1 and S4) [14–16,23].

3. Results

3.1. Neutron Transmittance of the Sample Cell and Toluene- d_8 Solution

An understanding of the neutron transmittance of the sample cell and upper layer solution is required for efficient experimental planning. For this reason, we first estimated the neutron transmittance of the sample cell and the upper-layer solution including the sample cell.

Figure 2 shows the experimental and calculated neutron transmittance of the sample cell and toluene- d_8 including the sample cell for the neutron beam with a wavelength range of 1.4–8.0 Å. It is natural that the neutron transmittance gradually increases with the decrease in neutron wavelength. The experimental and calculated transmittance values are in good agreement, despite minor differences. The mean neutron transmittance values of the sample cell and toluene- d_8 , including the sample cell, were estimated to be 90.6% and 13.4%, respectively. By removing the contribution of the sample cell, the neutron transmittance of toluene- d_8 was estimated to be 14.7%. This value is consistent with the expected transmittance value of 13.8%. Therefore, it can be concluded that the solvent of the upper layer must be deuterated to provide high neutron transmittance and that the measurement time of the neutron reflection using the sample cell can be predicted by the expected neutron transmittance value of the upper layer solvent.

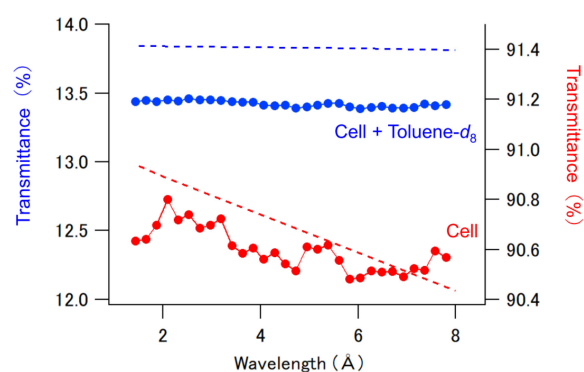


Figure 2. The transmittance dependence on the wavelength of the incident neutrons. The red circles are the transmittance of the sample cell and the blue circles are the transmittance of the toluene- d_8 including the sample cell. The dashed lines are the calculated transmittance values for each sample.

3.2. Measurements of Neutron Reflection from Air–Liquid Interfaces

Initially, to confirm the measurement accuracy of the sample cell system, NR profiles were obtained from the air–organic and air- D_2O solution interfaces.

Figure 3A shows the NR profiles at the air–organic and air–D₂O interfaces. All NR data showed a definite critical Q_c point. However, the air–toluene- h_8 reflectivity exhibited a quite rounded critical edge. It is possible that the data shape at the 0.006–0.008 \AA^{-1} region may not become smooth because the neutron beam intensity dropped dramatically in the endpoint region. Since the critical Q_c for total external reflection, defined as $(16\pi\rho)^{1/2}$, is sensitive to the SLD difference between the upper and lower layer, the measurement accuracy of the neutron reflection from the liquid interfaces can be evaluated by determining the SLD values of organic and aqueous liquids from the obtained Q_c points. Table S2 shows the parameters used to fit the measured NR profiles from the air–organic and air–D₂O solution interfaces. The obtained SLD and roughness values of three liquid samples, air–D₂O, air–toluene- h_8 and toluene- d_8 , were 6.28×10^{-6} and 4.1 \AA , 0.93×10^{-6} and 10.7 \AA and $5.60 \times 10^{-6} \text{ \AA}^{-2}$ and 9.8 \AA , respectively. As expected, the obtained SLD values agree with the predicted values (6.30×10^{-6} , 0.93×10^{-6} and $5.60 \times 10^{-6} \text{ \AA}^{-2}$). Therefore, it can be concluded that the sample cell system used in these experiments is suitable for measuring NR from aqueous and organic liquid surfaces. The obtained roughness value of the toluene- h_8 sample was bigger than that of the air–toluene- d_8 sample. This is probably owing to the isotopic effects of toluene- h_8 and toluene- d_8 . Note that the background level of the air–toluene- h_8 sample was higher than that of the air–toluene- d_8 sample and the background level was in the order of 4×10^{-6} . Thus, it can be suggested that the solvent for air–liquid interface reflection measurements must use deuterated solvents to provide low-background NR data.

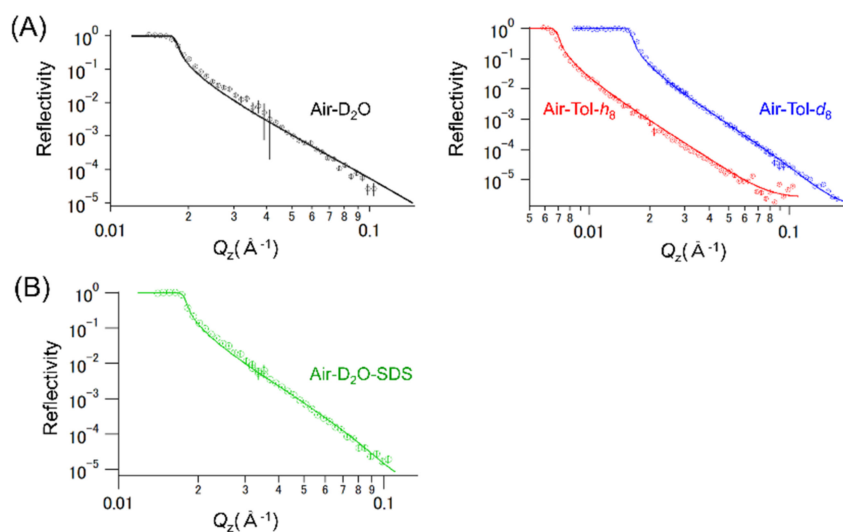


Figure 3. (A) NR profiles obtained from the air–organic and air–D₂O interfaces. (B) NR profiles obtained from the air–D₂O–SDS sample. RQ_z^4 vs. Q_z profiles are shown in Figure S2, and the fitting curves and the SLD profiles of the air–D₂O–SDS sample obtained by different models (Tables S3 and S5) are given in Figure S3.

In addition, we investigated the adsorption structures of SDS molecules on the air–D₂O surface using the sample cell system. Since SDS is a well-known surfactant and its adsorption structure at the air–water interface has been studied using the NR technique [23], it is suitable for exploratory experiments of air–liquid interface structure studies. Figure 3B shows the NR profiles obtained from the air–D₂O–SDS (10 mM) sample. The NR result is consistent with the assumption of an SDS layer with a thickness of 1.8 nm. Table S3 lists the parameters used to fit the measured NR profiles from the air–D₂O–SDS solution interface. The thickness, SLD and roughness values obtained from the NR analysis were 1.78 nm, $2.26 \times 10^{-6} \text{ \AA}^{-2}$ and 10.1 \AA , respectively. Because the length of an SDS molecule is $\sim 1.7 \text{ nm}$, this result indicates that an SDS monolayer was formed on the surface of the D₂O solution. This result is consistent with previous findings [23].

3.3. Measurements of Neutron Reflection from Liquid–Liquid Interfaces

To investigate the adsorption structure of SDS molecules on the toluene–water interface, NR profiles were obtained from the toluene- d_8 -D₂O and toluene- d_8 -D₂O-SDS (10 mM) interfaces using the sample cell system.

Figure 4A shows NR profiles obtained from the toluene- d_8 -D₂O and toluene- d_8 -D₂O-SDS samples. The NR data points are scattered due to the low reflection intensity at the liquid/liquid interface. The NR result is consistent with the assumption of an SDS layer with a thickness of ~1.2 nm. Table S3 shows the parameters used to fit the measured NR profiles from the toluene- d_8 -D₂O and toluene- d_8 -D₂O-SDS solution interfaces. The SLD values of each toluene- d_8 and D₂O solution obtained from the NR analysis were $5.72 \times 10^{-6} \text{ \AA}^{-2}$ and $6.20 \times 10^{-6} \text{ \AA}^{-2}$, respectively, for the toluene- d_8 -D₂O sample and $5.76 \times 10^{-6} \text{ \AA}^{-2}$ and $6.11 \times 10^{-6} \text{ \AA}^{-2}$, respectively, for the toluene- d_8 -D₂O-SDS sample. The thickness and SLD values of the adsorbed SDS layer obtained from the NR analysis were 1.23 nm and $4.43 \times 10^{-6} \text{ \AA}^{-2}$, respectively. This result not only indicates that SDS molecules adsorbed on the interface of the toluene- d_8 -D₂O solution, but also suggests that the adsorption structure of the SDS molecule was slightly different between the air–liquid and liquid–liquid interfaces. However, the obtained structure may not be completely accurate due to the limited Q_z -range of the NR data.

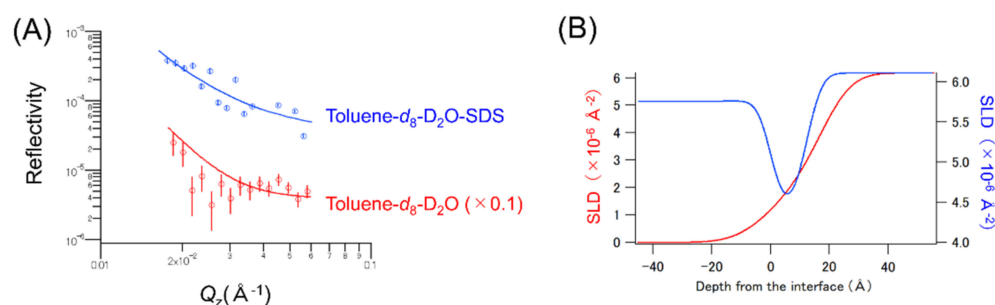


Figure 4. (A) NR profiles obtained from the toluene- d_8 -D₂O and toluene- d_8 -D₂O-SDS samples. The NR profiles of the toluene- d_8 -D₂O sample are vertically shifted to show the NR profiles more clearly. (B) The SLD profiles of the air-D₂O-SDS and toluene- d_8 -D₂O-SDS samples. The fitting curves and the SLD profiles of the air-D₂O-SDS sample obtained by different models (Tables S3 and S5) are given in Figure S4.

4. Discussion

There was a small difference in the surface roughness between the air–toluene- h_8 and air–toluene- d_8 samples. As mentioned above, this was probably owing to the isotopic effects of toluene- h_8 and toluene- d_8 . From previous reports related to the roughness of a thermally perturbed interface [24,25], the mean square roughness of the liquid–vapor interface can be expressed as

$$\sigma^2 = \sigma_0^2 + \frac{k_B T}{2\pi\gamma} \ln\left(\frac{2Q_{\max}}{Q\Delta\beta}\right) \quad (1)$$

where σ_0 is the intrinsic width of the interface, k_B is the Boltzmann constant, T is the temperature, γ is the interfacial tension of the liquid–vapor interface, Q_{\max} ($\cong \pi/a$, where a is the molecular diameter) is the short wavelength cutoff of the capillary waves and $\Delta\beta$ is the angular acceptance of the detector. H₂O/D₂O and other- h/d molecules have slightly different molecular size and chemical/kinetic properties [26–30]. In particular, deuteration of toluene results in a change in molar volume and surface tension from 106.28 (mL/mol) and 28.51 (mN/m) to 105.98 (mL/mol) and 28.4 (mN/m). Thus, it is reasonable to suppose that the interfacial tension and molecular sizes are slightly different between hydrogenated and deuterated toluene. Since the interfacial tension and molecular size of deuterated toluene are smaller than those of the hydrogenated toluene, the surface roughness of the air–toluene- d_8 sample decreased owing to their synergistic effect.

In the results of the SDS adsorption structure studies, there were small differences in the SDS adsorption layer structure on the air-D₂O and toluene-*d*₈-D₂O interfaces. Figure 4B shows the SLD profiles that led to the modeled reflectivity curves. Since the SLD is related to the volume fraction (φ), assuming that the SDS layer only contains the alkyl-chain moiety of adsorbing SDS, the determined SLD value can be used to deduce φ as follows [13]:

$$\varphi_s = (\rho - \rho_w)/(\rho_s - \rho_w) \quad (2)$$

where φ_s is the volume fraction of SDS, ρ_w is the SLD value of water (D₂O) and ρ_s is the SLD value of the SDS. The surface excess (in mol/area) of an SDS species, Γ_S , is given by [13,31–33]

$$\Gamma_S = \rho_s t \varphi_s / b_s N_A \quad (3)$$

where b_s is the scattering length of the SDS molecule and N_A is Avogadro's number. The obtained surface excess values were 4.75 (μmol/m²) for the air-D₂O-SDS sample; this result is consistent with the reference [13]. Therefore, it can be suggested that an SDS alkyl-chain exists in an extended conformation at the surface of water. On the other hand, recent interface structure studies of the SDS molecule suggested that the SDS headgroup is surrounded by water molecules, the SDS tail group does not interact strongly with *n*-hexadecane molecules and the SDS alkyl tail is in a disordered state and partially in contact with water [21]. In addition, in both experimental and simulation studies, similar phenomena were observed at the water-CCl₄-SDS sample interface [22,23] and the average length of the SDS molecule at the water-CCl₄ interface based on these findings was 1.33 nm. Considering the length of the SDS molecule (~1.7 nm), the layer thickness of the SDS molecule at the toluene-*d*₈-D₂O interface (1.23 nm) indicates that the SDS molecules would be in a disordered configuration in the SDS layer of the toluene-*d*₈-D₂O sample. Therefore, the difference in the adsorption structure of the SDS molecules between the air- and toluene-*d*₈-D₂O interfaces could be attributed to the difference in the adsorption behavior of the SDS molecules depending on the interfacial conditions. However, a rough depth resolution is given by $2\pi/Q_{\max}$ [34], which corresponds to ~3 nm in air-liquid sample measurements and ~10 nm in liquid-liquid sample measurements. Without any complementary data or special measurement methods, achieving a depth resolution of 1~2 nm using the NR method is extremely difficult. Additionally, the reproducibility of measurements obtained using various equipment and fitting analyses has been investigated in the X-ray reflectometry method [35]. The results revealed an inter-laboratory reproducibility of ~1 Å and a fitting analysis reproducibility of ~0.5 Å. In the NR software study, the same data were analyzed using different software [36]. Although these data were analyzed using Aurore and Motofit, starting from the same set of initial parameters, there was a 1~2 Å difference in the obtained optimized thickness values. Therefore, these results indicate that it is hard to believe that the reflectometry technique detects 1~2 nm thick layers with a sub-nm resolution. In conclusion, it must be noted that, for the fine estimation of the SDS layer thickness using the NR technique, additional information on the SDS layer thickness must be provided by complementary measurements, such as X-ray reflectometry or contrast variation experiments using deuterium-labeled compounds.

5. Conclusions

We introduce a new type of cell for liquid-liquid two-phase systems for NR measurements. The cell can keep an ideal liquid-liquid interface owing to a PTFE frame at the bottom, which also enables obtaining fine NR profiles regarding the interfacial structure. Using this new cell, we analyzed the adsorption structure of SDS molecules between toluene-*d*₈-D₂O and air-D₂O interfaces by the NR technique. A disordered configuration would be indicated for the SDS molecules in the SDS layer of the toluene-*d*₈-D₂O system, unlike those of the air-D₂O system. Additionally, for air-liquid interface reflection measurements, the use of deuterated solvents was preferable to obtain lower air-liquid interfacial roughness and low-background NR data.

This work indicates an effective method to understand the interfacial phenomena in liquid–liquid systems; therefore, the obtained results contribute to improving the analytical method of interfacial structures, leading to enhancing knowledge of chemical reactions in two-phase systems.

Supplementary Materials: The following are available online at <https://www.mdpi.com/article/10.3390/app12031215/s1>, Figure S1: Photos of a new type of cell with the PTFE frame. Figure S2: RQ_z^4 vs. Q_z profiles for the air–organic, air-D₂O, and air-D₂O-SDS samples. Figure S3: (A) The fitting curves of the air-D₂O-SDS sample as calculated using the model shown in Tables S3 and S5, and no SDS adsorbs model. (B) The SLD profiles of the air-D₂O-SDS sample as calculated using the model shown in Tables S3 and S5, and no SDS adsorbs model. Figure S4: (A) The fitting curves of the toluene-*d*₈-D₂O-SDS sample as calculated using the model shown in Tables S3 and S5, and no SDS adsorbs model. (B) The SLD profiles of the toluene-*d*₈-D₂O-SDS sample as calculated using the model shown in Tables S3 and S5, and no SDS adsorbs model. Table S1: The list of the constrained parameters for the model analysis of air-D₂O-SDS and toluene-*d*₈-D₂O-SDS samples. Table S2: The parameters used to fit the measured NR profiles from the air–organic and air-D₂O solution interfaces. Table S3: The parameters used to fit the measured NR profiles from the air-D₂O, air-D₂O-SDS, toluene-*d*₈-D₂O, and toluene-*d*₈-D₂O-SDS solution interfaces. Table S4: The list of the constrained parameters for the model analysis of air-D₂O-SDS and toluene-*d*₈-D₂O-SDS samples. Table S5: The parameters used to fit the measured NR profiles from the air-D₂O-SDS, and toluene-*d*₈-D₂O-SDS solution interfaces.

Author Contributions: Conceptualization, K.A.-S., N.L.Y., R.M. and H.N.; methodology, K.A.-S., N.L.Y. and R.M.; validation, K.A.-S., N.L.Y. and Y.U.; formal analysis, K.A.-S.; investigation, K.A.-S., Y.U., R.M. and H.N.; resources, K.A.-S. and H.N.; data curation, K.A.-S.; writing—original draft preparation, K.A.-S.; writing—review and editing, K.A.-S., N.L.Y., Y.U., R.M. and H.N.; supervision, K.A.-S. and N.L.Y.; project administration, K.A.-S. and N.L.Y.; funding acquisition, K.A.-S. and H.N. All authors have read and agreed to the published version of the manuscript.

Funding: The authors acknowledge financial support from the Japan Society of the Promotion of Science (JSPS) Grant-in-Aid for Scientific Research (B) 17H03438, (B) 20H02497, and (C) 21K05121.

Institutional Review Board Statement: Not applicable.

Informed Consent Statement: Not applicable.

Data Availability Statement: The data presented in this study are available on request from the corresponding author.

Acknowledgments: We thank H. Tanida (JAEA) for his support in the development of the sample cell. The NR samples were prepared at the User Experiment Preparation LabIII (CROSS). The neutron experiments were conducted at the BL16 SOFIA and BL17 SHARAKU apparatus in J-PARC, Tokai, Japan (Proposal Nos. 2018I1605, 2019I1606, 2020I1614 and 2020B0005).

Conflicts of Interest: The authors declare no conflict of interest.

References

- Scoppola, E.; Watkins, E.B.; Campbell, R.A.; Konovalov, O.; Girard, L.; Dufrêche, J.-F.; Ferru, G.; Fragneto, G.; Diat, O. Solvent Extraction: Structure of the Liquid–Liquid Interface Containing a Diamide Ligand. *Angew. Chem. Int. Ed.* **2016**, *55*, 9326–9330. [[CrossRef](#)]
- Zarbakhsh, A.; Querol, A.; Bowers, J.; Yaseen, M.; Lu, J.R.; Webster, J.R.P. Neutron Reflection from the Liquid–Liquid Interface: Adsorption of Hexadecylphosphorylcholine to the Hexadecane–Aqueous Solution Interface. *Langmuir* **2005**, *21*, 11704–11709. [[CrossRef](#)]
- Nishi, N.; Uruga, T.; Tanida, H. Potential dependent structure of an ionic liquid at ionic liquid/water interface probed by X-ray reflectivity measurements. *J. Electroanal. Chem.* **2015**, *759*, 129–136. [[CrossRef](#)]
- Schlossman, M.L. Liquid–liquid interfaces: Studied by X-ray and neutron scattering. *Curr. Opin. Colloid Interface Sci.* **2002**, *7*, 235–243. [[CrossRef](#)]
- Tanida, H.; Nagatani, H.; Harada, M. Development of the total-reflection XAFS method for the liquid–liquid interface. *J. Phys. Conf. Ser.* **2007**, *83*, 012019.
- Tummino, A.; Scoppola, E.; Fragneto, G.; Gutfreund, P.; Maestro, A.; Dryfe, R.A.W. Neutron reflectometry study of the interface between two immiscible electrolyte solutions: Effects of electrolyte concentration, applied electric field, and lipid adsorption. *Electrochim. Acta* **2021**, *384*, 138336. [[CrossRef](#)]

7. Scoppola, E.; Micciulla, S.; Kuhrts, L.; Maestro, A.; Campbell, R.A.; Konovalov, O.V.; Fragneto, G.; Schneck, E. Reflectometry Reveals Accumulation of Surfactant Impurities at Bare Oil/Water Interfaces. *Molecules* **2019**, *24*, 4113. [[CrossRef](#)]
8. Darwish, T.A.; Luks, E.; Moraes, G.; Yepuri, N.R.; Holden, P.J.; James, M. Synthesis of deuterated [D₃₂]oleic acid and its phospholipid derivative [D₆₄]dioleoyl-sn-glycero-3-phosphocholine. *J. Label Compd. Radiopharm.* **2013**, *56*, 520–529. [[CrossRef](#)]
9. Akutsu-Suyama, K.; Cagnes, M.; Tamura, K.; Kanaya, T.; Darwish, T.A. Controlled deuterium labelling of imidazolium ionic liquids to probe the fine structure of the electrical double layer using neutron reflectometry. *Phys. Chem. Chem. Phys.* **2019**, *21*, 17512–17516. [[CrossRef](#)]
10. Sun, H.; Zielinska, K.; Resmini, M.; Zarbakhsh, A. Interactions of NIPAM nanogels with model lipid multi-bilayers: A neutron reflectivity study. *J. Colloid Interface Sci.* **2019**, *536*, 598–608. [[CrossRef](#)]
11. Akutsu, K.; Cagnes, M.; Niizeki, T.; Hasegawa, Y.; Darwish, T.A. Penetration behavior of an ionic liquid in thin-layer silica coating: Ionic liquid deuteration and neutron reflectivity analysis. *Physical B* **2018**, *551*, 262–265. [[CrossRef](#)]
12. Penfold, J.; Tucker, I.; Thomas, R.K.; Zhang, J. Adsorption of Polyelectrolyte/Surfactant Mixtures at the Air–Solution Interface: Poly(ethyleneimine)/Sodium Dodecyl Sulfate. *Langmuir* **2005**, *21*, 10061–10073. [[CrossRef](#)]
13. Li, N.; Thomas, R.K.; Rennie, A.R. Effect of pH, surface charge and counter-ions on the adsorption of sodium dodecyl sulfate to the sapphire/solution interface. *J. Colloid Interface Sci.* **2012**, *378*, 152–158. [[CrossRef](#)]
14. de Aguiar, H.B.; Strader, M.L.; de Beer, A.G.F.; Roke, S. Surface Structure of Sodium Dodecyl Sulfate Surfactant and Oil at the Oil-in-Water Droplet Liquid/Liquid Interface: A Manifestation of a Nonequilibrium Surface State. *J. Phys. Chem. B* **2011**, *115*, 2970–2978. [[CrossRef](#)]
15. Conboy, J.C.; Messner, M.C.; Richmond, G.L. Investigation of Surfactant Conformation and Order at the Liquid-Liquid Interface by Total Internal Reflection Sum-Frequency Vibrational Spectroscopy. *J. Phys. Chem.* **1996**, *100*, 7617–7622. [[CrossRef](#)]
16. Schweighofer, K.J.; Essmann, U.; Berkowitz, M. Simulation of Sodium Dodecyl Sulfate at the Water-Vapor and Water-Carbon Tetrachloride Interfaces at Low Surface Coverage. *J. Phys. Chem. B* **1997**, *101*, 3793–3799. [[CrossRef](#)]
17. Takeda, M.; Arai, M.; Suzuki, J.; Yamazaki, D.; Soyama, K.; Maruyama, R.; Hayashida, H.; Asaoka, H.; Yamazaki, T.; Kubota, M.; et al. Current Status of a New Polarized Neutron Reflectometer at the Intense Pulsed Neutron Source of the Materials and Life Science Experimental Facility (MLF) of J-PARC. *Chin. J. Phys.* **2012**, *50*, 161–170.
18. Akutsu-Suyama, K. Fine-Structure Analysis of Perhydropolysilazane-Derived Nano Layers in Deep-Buried Condition Using Polarized Neutron Reflectometry. *Polymers* **2020**, *12*, 2180. [[CrossRef](#)]
19. Sakasai, K.; Satoh, S.; Seya, T.; Nakamura, T.; Toh, K.; Yamagishi, H.; Soyama, K.; Yamazaki, D.; Maruyama, R.; Oku, T.; et al. Materials and Life Science Experimental Facility at the Japan Proton Accelerator Research Complex III: Neutron Devices and Computational and Sample Environments. *Quantum Beam Sci.* **2017**, *1*, 10. [[CrossRef](#)]
20. Yamada, N.L.; Torikai, N.; Mitamura, K.; Sagehashi, H.; Sato, S.; Seto, H.; Sugita, T.; Goto, S.; Furusaka, M.; Oda, T.; et al. Design and performance of horizontal-type neutron reflectometer SOFIA at J-PARC/MLF. *Eur. Phys. J. Plus* **2011**, *126*, 108. [[CrossRef](#)]
21. Mitamura, K.; Yamada, N.L.; Sagehashi, H.; Torikai, N.; Arita, H.; Terada, M.; Kobayashi, M.; Sato, S.; Seto, H.; Goko, S.; et al. Novel neutron reflectometer SOFIA at J-PARC/MLF for in-situ soft-interface characterization. *Polym. J.* **2013**, *45*, 100–108. [[CrossRef](#)]
22. Nelson, A. Co-refinement of multiple-contrast neutron/X-ray reflectivity data using MOTOFIT. *J. Appl. Crystallogr.* **2006**, *39*, 273–276. [[CrossRef](#)]
23. Purcell, I.P.; Lu, J.R.; Thomas, R.K.; Howe, A.M.; Penfold, J. Adsorption of Sodium Dodecyl Sulfate at the Surface of Aqueous Solutions of Poly(vinylpyrrolidone) Studied by Neutron Reflection. *Langmuir* **1998**, *14*, 1637–1645. [[CrossRef](#)]
24. Ocko, B.M.; Wu, X.Z.; Sirota, E.B.; Sinha, S.K.; Deutsch, M. X-ray Reflectivity Study of Thermal Capillary Waves on Liquid Surfaces. *Phys. Rev. Lett.* **1994**, *72*, 242–245. [[CrossRef](#)]
25. Bowers, J.; Zarbakhsh, A.; Webster, J.R.P.; Hutchings, L.R.; Richards, R.W. Neutron Reflectivity Studies at Liquid–Liquid Interfaces: Methodology and Analysis. *Langmuir* **2001**, *17*, 140–145. [[CrossRef](#)]
26. Bartell, L.S.; Kuchitsu, K.; deNeui, R.J. Mean and Equilibrium Molecular Structures of Methane and Deuteromethane as Determined by Electron Diffraction. *J. Chem. Phys.* **1961**, *35*, 1211–1218. [[CrossRef](#)]
27. Bartell, L.S.; Roskos, R.R. Isotope Effects on Molar Volume and Surface Tension: Simple Theoretical Model and Experimental Data for Hydrocarbons. *J. Chem. Phys.* **1966**, *44*, 457–463. [[CrossRef](#)]
28. Wade, D. Deuterium isotope effects on noncovalent interactions between molecules. *Chem.-Biol. Interact.* **1999**, *117*, 191–217. [[CrossRef](#)]
29. Dunitz, J.; Ibberson, R.M. Is Deuterium Always Smaller than Protium? *Angew. Chem. Int. Ed.* **2008**, *47*, 4208–4210. [[CrossRef](#)]
30. Rolle, M.; Jin, B. Normal and Inverse Diffusive Isotope Fractionation of Deuterated Toluene and Benzene in Aqueous Systems. *Environ. Sci. Technol. Lett.* **2017**, *4*, 298–304. [[CrossRef](#)]
31. Campbell, R.A.; Arteta, M.Y.; Angus-Smyth, A.; Nylander, T.; Varga, I. Effects of Bulk Colloidal Stability on Adsorption Layers of Poly(diallyldimethylammonium Chloride)/Sodium Dodecyl Sulfate at the Air-Water Interface Studied by Neutron Reflectometry. *J. Phys. Chem. B* **2011**, *115*, 15202–15213. [[CrossRef](#)]
32. Braun, L.; Uhlig, M.; von Klitzing, R.; Campbell, R.A. Polymers and surfactants at fluid interfaces studied with specular neutron reflectometry. *Adv. Colloid Interface Sci.* **2017**, *247*, 130–148. [[CrossRef](#)]
33. Campbell, R.A. Recent advances in resolving kinetic and dynamic processes at the air/water interface using specular neutron reflectometry. *Curr. Opin. Colloid Interface Sci.* **2018**, *37*, 49–60. [[CrossRef](#)]

34. Pannetier, M.; Doan, T.D.; Ott, F.; Berger, S.; Persat, N.; Fermon, C. Polarised neutron reflectometry for GMR sensors optimization. *Europhys. Lett.* **2003**, *64*, 524–528.
35. Colombi, P.; Agnihotri, D.K.; Asadchikov, V.E.; Bontempi, E.; Bowen, D.K.; Chang, C.H.; Depero, L.E.; Farnworth, M.; Fujimoto, T.; Gibaud, A.; et al. Reproducibility in X-ray reflectometry: Results from the first world-wide round-robin experiment. *J. Appl. Cryst.* **2008**, *41*, 143–152. [[CrossRef](#)]
36. Gerelli, Y. Aurore: New software for neutron reflectivity data analysis. *J. Appl. Cryst.* **2016**, *49*, 330–339. [[CrossRef](#)]